Agricultural and Forest Meteorology 311 (2021) 108673

Contents lists available at ScienceDirect

Agricultural and Forest Meteorology

journal homepage: www.elsevier.com/locate/agrformet

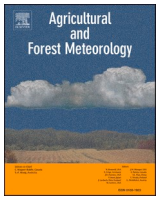

Assessing maize potential to mitigate the adverse effects of future rising temperature and heat stress in China

Mingxia Huang [a,b], Jing Wang [a,*], Bin Wang [b,c,**], De Li Liu [b,d], Puyu Feng [e], Qiang Yu [c,f,g], Xuebiao Pan [a], Cathy Waters [h]

[a] College of Resources and Environmental Sciences, China Agricultural University, Beijing 100193, China
[b] NSW Department of Primary Industries, Wagga Wagga Agricultural Institute, NSW 2650, Australia
[c] State Key Laboratory of Soil Erosion and Dryland Farming on the Loess Plateau, Northwest A&F University, Shaanxi 712100, China
[d] Climate Change Research Centre, University of New South Wales, NSW 2052, Australia
[e] College of Land Science and Technology, China Agricultural University, Beijing 100193, China
[f] College of Resources and Environment, University of Chinese Academy of Science, Beijing 100049, China
[g] School of Life Sciences, Faculty of Science, University of Technology Sydney, NSW 2007, Australia
[h] NSW Department of Primary Industries, 34 Hampden Street, Dubbo, NSW 2830, Australia

ARTICLE INFO

Keywords:
Climate change
Adaptation options
China's Maize Belt
CERES-Maize model
Cropping system

ABSTRACT

Rising temperatures and frequent extreme high temperature events under future climate scenarios have posed pressing challenges with respect to global food security. Previous climate-crop modelling studies have investigated the impacts of rising temperature and heat stress on grain yield. However, the potential and priority of dealing with rising mean temperature or heat stress using genetically different cultivars have not been identified. We investigated the impacts of climate change on maize yield across China's Maize Belt (23°–48°N) using the CERES-Maize model driven by future climate scenarios under contrasting maize growing season temperatures of 18–24°C during the 2050s (2040–2069) and the 2080s (2070–2099). We also assessed the potential of different cultivars to adapt to rising temperatures and heat stress with an extreme hot global climate model from CMIP6 under a high emission scenario (SSP585). Our simulated results indicated that the shortened growth period resulting from rising temperatures, decreased photosynthesis caused by heat stress, and decreased grain-filling rate due to heat stress were the main reasons causing future maize (*Zea mays* L.) yield decreases in all subregions of China's Maize Belt. The priority applied to using a cultivar with a longer growth period or higher heat-tolerance to cope with climate warming depends on the particulars of the local climate and cropping system. Specifically, the potential for adapting to rising temperature is generally higher than the potential for adapting to heat stress in all subregions except the North China Plain (NCP) where the potential for adapting to heat stress is higher than the potential for adapting to rising temperature. Our study demonstrated the necessity of using cultivars with appropriate traits to alleviate the adverse effects of climate warming. Also, our findings provide important information for the direction and priority of future breeding in different climate regions with various cropping systems across China's Maize Belt.

1. Introduction

Global population has been increasing rapidly in recent decades and is projected to exceed 9.7 billion by 2050 (UN_DESA, 2017), leading to increasing food demand. Meanwhile, rapid urban expansion has been shrinking cropland area throughout the world (van Vliet et al., 2017). The imbalance between food supply and demand puts great pressure on global food security. Increasing yield per hectare, especially with regard to cereal crops, is an important means to combat the food crisis. However, crop yields have been adversely affected by climate change, specifically climate warming (Huang et al., 2020; Lobell et al., 2011a). Therefore, how to effectively mitigate the adverse effects of climate warming and boost yield potential by developing a robust adaptation strategy is critical in order to maintain global food security (Challinor

* Corresponding author at: College of Resources and Environmental Sciences, China Agricultural University, Beijing 100193, China.
** Corresponding author at: NSW Department of Primary Industries, Wagga Wagga Agricultural Institute, NSW 2650, Australia.
E-mail addresses: wangj@cau.edu.cn (J. Wang), bin.a.wang@dpi.nsw.gov.au (B. Wang).

https://doi.org/10.1016/j.agrformet.2021.108673
Received 2 December 2020; Received in revised form 4 August 2021; Accepted 7 October 2021

et al., 2016; Guan et al., 2017).

Climate warming is characterized by the rising average temperature of the Earth's climate system (IPCC, 2014), resulting in more frequent and intensified temperature extremes (Deryng et al., 2014; Gourdji et al., 2013). Rising temperature shortened the period of biomass accumulation by accelerating crop development, resulting in decreased grain yield (Asseng et al., 2014; Challinor et al., 2016). As one of the most important grain and feeding crops, global maize (*Zea mays* L.) yield was estimated to decrease by 3.8% during 1980–2008 due to climate change (especially due to rising temperatures) (Hawkins et al., 2013; Lobell et al., 2011a; Schauberger et al., 2017). In addition, intensified heat stress occurring at the reproductive period has decreased maize yields by damaging several physiological processes of maize, including photosynthesis, pollination, and kernel grain filling related to kernel number and kernel size (Lizaso et al., 2018; Rattalino Edreira and Otegui, 2012; Sanchez et al., 2014).

China accounts for 18.6% of global total maize production (FAO, 2017), and is the second largest maize producer in the world. Therefore, maize in China plays an important role in the global maize market. Multiple global climate models (GCMs) from the Coupled Model Intercomparison Project 5 (CMIP5) projected that mean temperature and the frequency and intensity of extreme high temperature will increase continuously over the globe in the future (Ben-Ari et al., 2018; Kang and Eltahir, 2018; Trnka et al., 2014). Additionally, more frequent heatwaves are projected in China, with more high temperature days (daily average temperature over 30°C) in the far future than in the historical period (Li et al., 2019). Without adaptation, maize yield has been predicted to decrease by 3.9%–26.6% with climate warming of 3°C in China's maize planting regions (Lobell et al., 2011b).

Selecting adapted cultivars is recognized as one of the most effective measures to address both rising temperature and heat stress (Challinor et al., 2016; Challinor et al., 2007; Chisanga et al., 2020b). For example, selecting cultivars with longer growth periods had a great potential to alleviate the negative impact of rising temperature on crop growth period (Huang et al., 2020; Tao et al., 2014). Meanwhile, using heat-tolerant cultivars can mitigate the adverse impacts of heat stress on photosynthesis and grain-filling of maize (Challinor et al., 2007; Rattalino Edreira and Otegui, 2012; Tesfaye et al., 2016; Zhang and Zhao, 2017). Over the last few decades, maize breeders have already targeted specific crop traits to breed new cultivars for better mitigating climate change impacts (Cairns et al., 2012). However, the true potential of new cultivars with different genotypes to address the negative effects of future climate change remains unclear. The use of process-based crop models is a common method for evaluating the relative potential of adaptation strategies. For example, using the Agricultural Production Systems sIMulator (APSIM) model, Xiao et al. (2020b) designed different traits of maize ideotypes planted at various dates to maximize yield and water use efficiency (WUE) under future climate conditions in the North China Plain (NCP). Their simulated results showed that maize ideotypes under future climate should have a longer reproductive growth period, faster potential grain filling rate, larger maximum grain number, and higher radiation use efficiency. In addition, Zhang and Zhao (2017) found that using heat-tolerant cultivars can increase maize yield by 6%–10% in the NCP compared with using heat-susceptible ones.

The majority of previous studies assessed the contributions of selecting cultivars with different maize genotypes to adapt to future climate warming (Abbas et al., 2017; Guan et al., 2017; Huang et al., 2020). However, few studies evaluated the potential to mitigate the adverse effects of rising temperature and heat stress on maize yields. In addition, no study has provided the priority on targeting where and when adapted cultivars with higher thermal time or higher heat-tolerance could better adapt to future climate change. This is very important because such information will provide essential reference points for plant breeders and policy makers to develop practical solutions to cope with global climate change. The objectives of our study were to 1) test the performance of the CERES-Maize model across China's Maize Belt, 2) evaluate the relative potential of adaptation options by adjusting thermal time and increasing heat-tolerance of maize cultivars in the calibrated CERES-Maize model, 3) provide useful information for developing cultivar adaptation strategies in different regions of China's Maize Belt.

2. Materials and methods

2.1. Study region

China's Maize Belt was divided into six maize planting regions (Fig. 1) based on geographic locations and cropping systems (Table 1) (Huang et al., 2020). In total, 163 weather stations located in the six maize planting regions were selected as the study sites used in the simulations. Regions I–V had a temperate monsoon climate while region VI had a subtropical monsoon climate. The single maize cropping system is dominant in regions I–IV, with the maize growing season running from May to September, while the wheat (*Triticum aestivum* L.)-maize rotation is widely used in region V, with the maize growing season running from June to September (Table 1). For region VI, the wheat-maize relay intercropping system is popular, with the maize growing season running from April to September. Across China's Maize Belt, growing season mean temperature varies between 18.0–24.2°C with the highest and lowest values in region V and I (Table S1), respectively. Growing season total precipitation varies between 428–928 mm, with the highest and lowest values in region VI and IV (Table S1), respectively. Growing season mean solar radiation varies between 14.5–17.7 MJ m^{-2}, with the highest and lowest values in region IV and region VI (Table S1), respectively.

2.2. Sources of weather data

The weather data for each site during 1980–2016 included daily precipitation (mm), maximum temperature (°C), minimum temperature (°C), and sunshine hours (h), and were obtained from the China Meteorological Administration (CMA). Daily solar radiation (MJ $m^{-2}d^{-1}$) was calculated using the Angstrom equation by sunshine hours (Wang et al., 2015). CMA has conducted quality control by checking the homogeneity and reliability of climate data before they were released (Wang et al., 2020).

2.3. Crop and soil data

Observed maize phenological data during 1980–2011 were collected from 100 agro-meteorological observation sites to provide a reference for setting maize planting and harvest dates (Fig. 1 and Table 1). Observed experimental data on maize cultivar, phenology (e.g., planting, flowering, and maturity dates), yield, and field management practices (e.g., planting density, irrigation, and N fertilization amount) from the six experimental sites were used to calibrate and validate the maize model (Fig. 1, Table 2). Detailed information regarding soil and climate data for each experimental site is shown in Table S2 and Table S3, respectively. Field experimental data for regions I, III, and VI were extracted from tables or figures in the published literature using WebPlotDigitizer software (https://automeris.io/WebPlotDigitizer/). Field experimental data for regions II and IV were obtained from agro-meteorological observation sites, and field experimental data in region V were sourced from serial planting experiments in 2017 and 2018 at the Hebi experimental site in Henan province of the NCP. At each maize planting region, one typical soil type was selected with detailed information from the China Soil Scientific Database (Table S2).

2.4. Baseline and future climate scenarios

Historical and future climate data (including daily maximum and minimum temperatures, daily precipitation, and daily solar radiation)

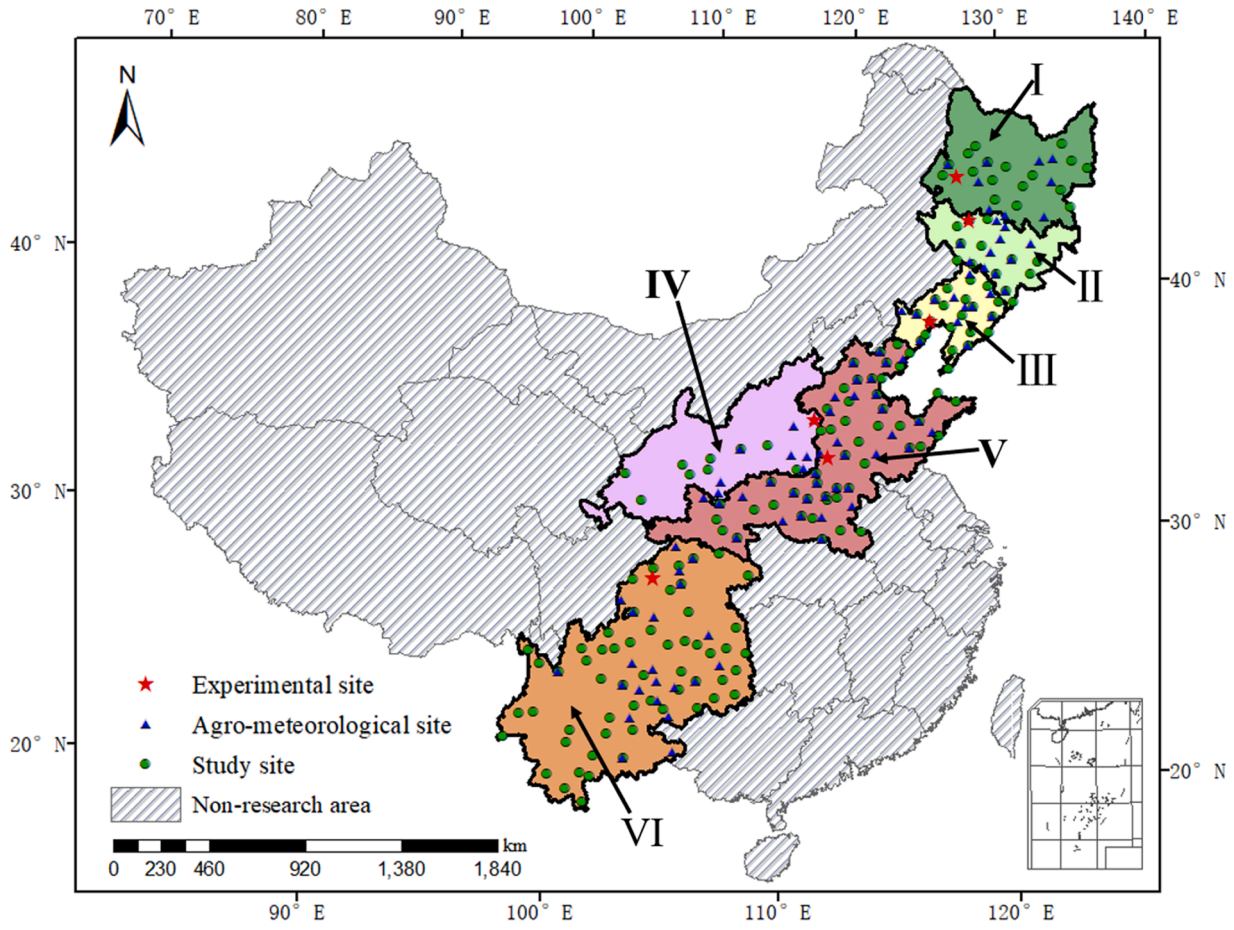

Fig. 1. Geographic location of six planting regions across China's Maize Belt and the distribution of 163 weather stations, 100 agro-meteorological sites, and six experimental sites.

Table 1
Division of the maize planting regions and cropping systems across China's Maize Belt.

Region	Location	Cropping system	Growing season	Number of weather stations	Number of agro-meteorological sites	Number of experimental sites
I	Northeast China	Single	1/May–30/Sep	17	10	1
II	Northeast China	Single	1/May–30/Sep	12	11	1
III	Northeast China	Single	1/May–30/Sep	20	13	1
IV	Northwest China	Single	1/May–30/Sep	9	8	1
V	North China Plain	Double	1/June–30/Sep	49	36	1
VI	Southwest China	Mixed	1/Apr–30/Sep	56	22	1

from 1961 to 2100 were statistically downscaled from monthly gridded climate data simulated by 20 global climate models (GCM) under high Shared Socio-Economic Pathways (SSP585) (https://tntcat.iiasa.ac.at/SspDb/dsd?Action=htmlpage&page=50) from the Coupled Model Intercomparison Project 6 (CMIP6) with the NWAI-WG downscaling model (Liu and Zuo, 2012). The gridded monthly climate data were downscaled to site level using the spatial inverse distance-weighted (IDW) interpolation method. Bias for monthly data was corrected using the Q-Q plotting approach by comparing the GCM projected and observed climatic data. Then, bias-corrected monthly data were downscaled to daily scale with the modified WGEN stochastic weather generator (Liu and Zuo, 2012). The downscaled climate data had good performance in reproducing observations, and a detailed test of our statistical downscaling method has been done by Liu and Zuo (2012) and Liu et al. (2017). Climate outputs based on this downscaling approach have been extensively applied in climate change impact studies in China (Bai et al., 2020; Xiao et al., 2020a). To identify the adaptation potential of maize to extreme temperature in this study, we selected one of 20 GCMs from CMIP6 that had the highest temperature projected in the future for China's Maize Belt (Fig. S1). The CanESM5 model can reproduce historical climate change over the globe (Guo et al., 2021; Swart et al., 2019; Yazdandoost et al., 2021). We used a Q-Q plot to compare observed and downscaled climate projected by CanESM5 across China's Maize Belt (Fig. S2). The results indicated a good match between observed and projected climate for the study area, as the points generally followed the 1:1 line and the NRMSEs were low. Our study periods were divided as the baseline period (1980–2009), the 2050s (2040–2069), and the 2080s (2070–2099). The baseline climate for all regions is shown in Table S1.

2.5. DSSAT-CERES-Maize model and its parameterization

The CERES-Maize model is a part of the Decision Support System for Agro-Technology Transfer (DSSAT), and is a mechanistic crop growth model that can simulate daily maize growth and development. The model includes four sub-modules (i.e., weather, soil, plant, and

Table 2
Detailed information for field experiments used to calibrate and validate the CERES-Maize model.

Experimental site	Cultivar	Climate type	Soil type	Treatment	Planting dates (day/month/year)	Planting density (plant m^{-2})	N fertilization amount (kg ha^{-1})	Irrigation amount (mm)	Observed data	Experimental data source
Lindian	Zhedan37	Temperate monsoon climate	Black soil	Planting date	27/4/2012, 7/5/2012, 17/5/2012, 8/5/2013, 15/5/2013, 22/5/2013	6.15	82.5	0	Flowering date, Maturity date, Grain yield	Han et al. (2016)
Qianguo	Jidan180	Temperate monsoon climate	Black soil	none	3/5/2002, 27/4/2003, 6/5/2004, 28/4/2005, 6/5/2006	6.75	180	0	Flowering date, Maturity date, Grain yield	Agro-meteorological site
Jinzhou	Danyu39	Temperate monsoon climate	Black soil	Planting date	20/4/2012, 30/4/2012, 10/5/2012, 20/4/2013, 30/4/2013, 10/5/2013	4.2	80	0	Flowering date, Maturity date, Grain yield	Huang et al., 2020
Xiyang	Nongda108	Semi-arid continental climate	Fluvio-aquatic soil	none	2/5/2003, 28/4/2004, 30/4/2005, 2/5/2006, 4/5/2007, 6/5/2008	6.75	180	0	Flowering date, Maturity date, Grain yield	Agro-meteorological site
Hebi	Zhengdan958	Semi-arid monsoon climate	Cinnamon soil	Planting date	10/6/2017, 15/6/2017, 10/6/2018, 15/6/2018	6.75	150	30	Flowering date, Maturity date, Grain yield	This study
Zhongjiang	Zhenghong505	Subtropical monsoon climate	Lithologic soil	Planting date	25/3/2015, 10/4/2015, 25/4/2015, 25/3/2016, 10/4/2016, 25/4/2016, 10/5/2016, 25/5/2016	4.95	225	0	Flowering date, Maturity date, Grain yield	Dou et al. (2017)

management modules) (Araya et al., 2015; Chisanga et al., 2020a; Ruane et al., 2013). Climate, soil, genotype, and agronomic management data are essential inputs for CERES-Maize (Jones et al., 2003). Table S4 lists the required input data for running the model. DSSAT v4.7 was used in our study, and the model was implemented in R 3.5.2 for batch simulation.

In CERES-Maize, phenological development is divided into eight stages, including planting to germination, germination to emergence, emergence to end of juvenile phase (EndJuv), EndJuv to tassel initiation (Tl), Tl to end of leaf growth (EndLf), EndLf to grain filling (GF), and GF to maturity (Jones et al., 2003). The period from planting to germination is set as one day, while the period from germination to emergence is determined by planting depth and thermal time needed for growing a centimeter of stem. The stage from emergence to physiological maturity is determined by thermal time (P1, P5) computed as the sum of three-hourly mean temperatures above the base temperature, while the stages from EndJuv to Tl and from Tl to GF are also impacted by photoperiod sensitivity (P2) and Phyllochron interval (PHINT), respectively. Daily potential biomass accumulation is calculated by daily solar radiation interception and radiation use efficiency (RUE), while actual daily biomass accumulation is reduced from daily potential biomass accumulation by the stresses of water, nitrogen, and heat. The final grain yield of maize is determined by final grain number, actual grain filling rate, and re-translocation from aboveground biomass. Final grain number is determined by potential number of kernels per plant (G2) and accumulated biomass from EndLf to GF. Final actual grain filling rate is determined by potential kernel filling rate (G3) and daily mean temperature from GF to maturity.

To minimize the spatial heterogeneity of maize cultivars, a representative cultivar was selected for each of the six planting regions (Table 2). Genetic parameters for all cultivars were derived by a "trial-and-error" method based on maize growth and development data from agro-meteorological observation sites and field experiments (Table 2). Observed flowering and maturity dates were used to derive genetic parameters of maize phenology (P1, P2, P5, PHINT), and observed maize yield was used to derive genetic parameters for maize yields (G2, G3). Based on different years and planting dates, all experimental data were separated into two independent groups for calibration and validation of the CERES-Maize model (Table S5). Supporting information Text T1 shows the statistical metrics for model evaluation.

2.6. Long-term simulation setup

To evaluate the impacts of climate change on maize yield and adaption potential of modified cultivars, we conducted long-term simulations under rainfed conditions and under potential conditions without any nitrogen stress. The initial soil water content was reset at 30% of plant available water holding capacity (PAWC) for regions I–V and at 81% of PAWC for region VI every year, according to the observed historical average initial soil water content before planting recorded from agro-meteorological observation sites. For all regions, maize planting density was set as 67,500 plants ha^{-1}, with plant row spacing and depth of 60 cm and 5 cm, respectively. For all regions, planting date was set as the historical average planting date recorded in agro-meteorological sites. Maize was harvested at physiological maturity, or the day before the first frost day calculated as the daily minimum

temperature below 0°C for regions I–IV with the single-cropping system, or three days before planting the next season crop for regions V–VI with the double-cropping system. In addition, yearly rising CO_2 concentration (Huang et al., 2020) was used as an input for CERES-Maize to consider the effects of elevated CO_2 on maize transpiration rate and potential growth rate (Webber et al., 2017).

CERES-Maize has been widely used to evaluate the impacts of climate change on maize (Braga et al., 2008; Lin et al., 2017; Yakoub et al., 2017). Singh et al. (2014) modified the lower and upper optimum temperatures to improve the responses of photosynthesis and grain filling rate to heat stress in CERES-Maize. We used this modified version of CERES-Maize in our study.

Rising temperatures were reported to reduce biomass accumulation by shortening the maize growth period (Lin et al., 2017), while heat stress was seen to reduce maize yield mainly by decreasing photosynthesis and grain filling rate (López-Cedrón et al., 2005; Singh et al., 2014). The impacts of heat stress on maize photosynthesis and grain filling rate were calculated using a piecewise function in CERES-Maize:

$$I_{T,Pho} = \begin{cases} 0 \; for \; T_{mean} \le 6.2 \; or \; T_{mean} > 44 \\ \dfrac{(T_{mean} - 6.2)}{10.3} \; for \; 6.2 < T_{mean} \le 16.5 \\ 1 \; for \; 16.5 < T_{mean} \le 33 \\ \dfrac{(44 - T_{mean})}{11} \; for \; 33 \; < T_{mean} \le 44 \end{cases}, \quad (1)$$

$$I_{T,GFR} = \begin{cases} 0 \; for \; T_{mean} \le 5.5 \; or \; T_{mean} > 35 \\ \dfrac{(T_{mean} - 5.5)}{10.5} \; for \; 5.5 < T_{mean} \le 16 \\ 1 \; for \; 16 < T_{mean} \le 27 \\ \dfrac{(35 - T_{mean})}{8} \; for \; 27 \; < T_{mean} \le 35 \end{cases}, \quad (2)$$

where $I_{T,Pho}$ and $I_{T,GFR}$ are the impact indexes of heat stress on photosynthesis and grain filling rate respectively, ranging between 0 and 1. T_{mean} is the daily mean temperature. An index of 1 indicates no impact of heat stress, and a value of 0 indicates severe heat damage (Fig. 2).

The thermal time of adapted maize cultivars in CERES-Maize was generated by increasing P1 and P5 with a 10% increment based on the current maize cultivar because P1 and P5 were two important parameters that control maize phenology. The detailed combinations of P1 and P5 for each region are presented in Table S6.

The upper limits of optimal temperatures for photosynthesis ($T_{Pho}1$) and grain filling rate ($T_{GFR}1$), and lethal temperature thresholds for photosynthesis ($T_{Pho}2$) and grain filling rate ($T_{GFR}2$) were increased to explore the adaptation capacity of increasing heat-tolerance of maize to heat stress (Fig. 2). We modified the impact curves of temperature on photosynthesis and grain filling rate by increasing $T_{Pho}1$, $T_{GFR}1$, $T_{Pho}2$, and $T_{GFR}2$ from the original values of 33, 27, 44, and 35°C to new values of 40, 37, 51, and 45°C, respectively, with a step of 1°C. This modification assumed unchanged curve slope during $T_{Pho}1$ to $T_{Pho}2$ and $T_{GFR}1$ to $T_{GFR}2$ (Table S7).

As mentioned above, the adverse effect due to rising temperature was mainly reflected by shortened growth period, while decreased photosynthesis and grain-filling rates were due to heat stress. Therefore, we increased thermal time for each current maize cultivar to adapt to rising temperature. We changed the optimal thresholds for maize photosynthesis and grain filling rate to help maize adapt to heat stress. The simulation was operated via the following three steps:

(1) Rising temperature would shorten the maize growth period. We lengthened maize phenological development by increasing the thermal time of current maize cultivars within a maize growing season (Table 1) to investigate the potential of adapting to rising temperature.
(2) We increased temperature thresholds of photosynthesis and grain-filling rate based on the current cultivar to assess the potential of adapting to heat stress (Fig. 2).
(3) The potential of adapting to climate warming was achieved when maize yield was highest by increasing thermal time and temperature thresholds of photosynthesis and grain-filling rate.

By introducing appropriate adaption traits into the current cultivar, maize yield would increase due to its increased potential to cope with the negative impacts of climate warming. Optimal adaption traits were then obtained when maize yield was up to 95% of maximum yield.

To compare the accumulated effects of heat stress induced by different magnitudes of intensity and frequency of high temperature over maize planting regions, we calculated the accumulated impact factors of heat stress on photosynthesis ($F_{T,Pho}$) and grain filling rate ($F_{T,GFR}$):

$$F_{T,Pho} = \sum_{i=33}^{40} f_{T,Pho,i} \times d_i \Big/ D_{gp}, \quad (3)$$

$$F_{T,GFR} = \sum_{i=27}^{37} f_{T,GFR,i} \times d_i \Big/ D_{gf}, \quad (4)$$

where $f_{T,Pho,i} = 1 - I_{T,Pho,i}$, and (5)

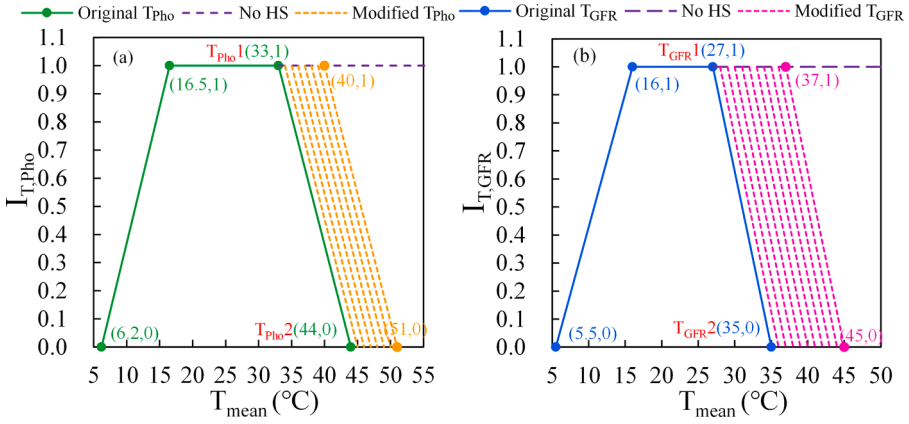

Fig. 2. Impact curves of daily mean temperature on photosynthesis (a) and grain filling rate (b) in the CERES-Maize model. "Original T_{Pho}" and "Original T_{GFR}" represent the impact curve of daily mean temperature on photosynthesis and grain filling rate, respectively, for the current cultivar. "No HS" represents no heat stress effect; "Modified T_{Pho}" and "Modified T_{GFR}" represent the impact curves of daily mean temperature on photosynthesis and grain filling rate, respectively.

$$f_{T,GFR,i} = 1 - I_{T,GFR,i}, \quad (6)$$

where $f_{T,Pho,i}$ and $f_{T,GFR,i}$ represent the effects of heat stress at temperature i on photosynthesis and grain filling rate, respectively; d_i represents the total days of temperature i; and D_{gp} and D_{gf} represent the total days of the growth period and grain filling period, respectively. For the convenience of calculation, all temperatures were rounded to the nearest integer in Eqs. (3)–(6), i.e., i=33 will account for 32.5 ≤ T< 33.5.

2.7. Data analysis

To assess the effect of climate change and the potential of adaptation options to climate warming (Guan et al., 2017), yield change due to climate change ($\triangle Y_{CC}$), adaptation potential to rising temperature ($\triangle P_{ART}$), adaptation potential to heat stress ($\triangle P_{AHT}$), and the combined adaptation potential to rising temperature and heat stress ($\triangle P_{ART\&AHT}$) were calculated as follows:

$$\Delta Y_{CC}(\%) = \frac{\left(Y_{2050s/2080s} - Y_{bl}\right)}{Y_{bl}} \times 100, \quad (7)$$

$$\Delta P_{ART}(\%) = \frac{\left(Y_{2050s/2080s,ART} - Y_{bl,ART}\right) - \left(Y_{2050s/2080s} - Y_{bl}\right)}{Y_{bl}} \times 100, \quad (8)$$

$$\Delta P_{AHT}(\%) = \frac{\left(Y_{2050s/2080s,AHT} - Y_{bl,AHT}\right) - \left(Y_{2050s/2080s} - Y_{bl}\right)}{Y_{bl}} \times 100, \quad (9)$$

$$\Delta P_{ART\&AHT}(\%) = \frac{\left(Y_{2050s/2080s,ART\&AHT} - Y_{bl,ART\&AHT}\right) - \left(Y_{2050s/2080s} - Y_{bl}\right)}{Y_{bl}} \times 100, \quad (10)$$

where $Y_{bl/2050s/2080s}$ represents yield during the baseline period, the 2050s, and the 2080s, respectively. $Y_{bl/2050s/2080s,\ ART}$ represents the yield with adaptation to cope with rising temperature during the baseline period, the 2050s, and the 2080s, respectively. $Y_{bl/2050s/2080s,\ AHT}$ represents the yield with adaptation to cope with heat stress during the baseline period, the 2050s, and the 2080s, respectively. $Y_{bl/2050s/2080s,\ ART\&AHT}$ represents the yield with adaptation to mitigate both rising temperature and heat stress during the baseline period, the 2050s, and the 2080s, respectively.

3. Results

3.1. Performance of the CERES-Maize model across China's Maize Belt

Fig. 3 shows the comparisons of observed and simulated maize flowering date, maturity date, and yield for a typical cultivar planted in each of the six planting regions. In general, CERES-Maize with adjusted genetic parameters (Table 3) exhibited good performance for simulating the periods of planting to flowering and planting to maturity. The root-mean-square errors (RMSE) were 2.9 and 2.3 days for flowering, and 4.2 and 4.5 days for maturity for the calibration and validation datasets, respectively (Fig. 3). Additionally, the observed and simulated maize yields showed good agreement with R^2 values of 0.83 for the calibration period and 0.82 for the validation period. The RMSE (NRMSE) was 1.0 ha^{-1} (11.7%) for the calibration period while the RMSE (NRMSE) was

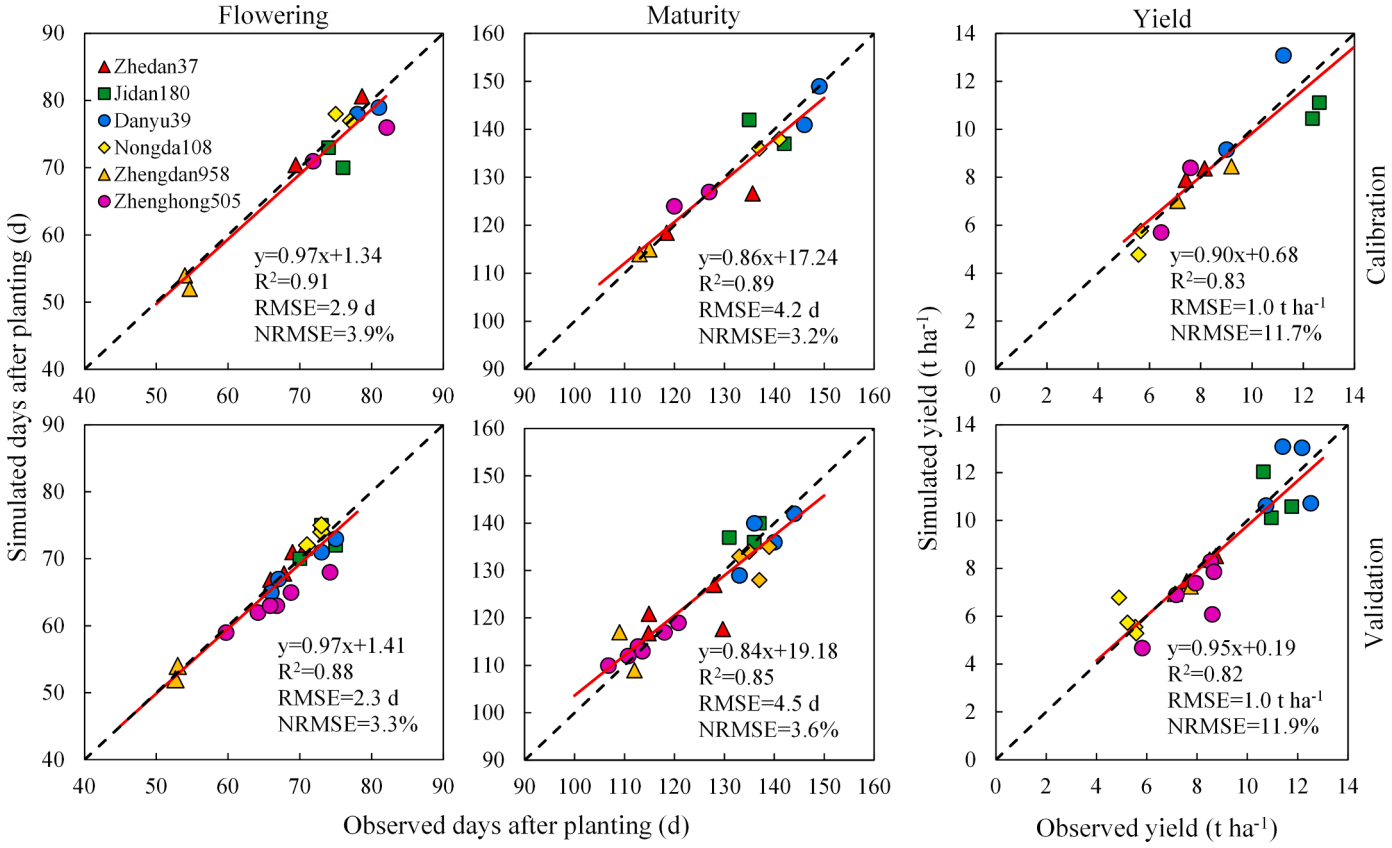

Fig. 3. Comparison of simulated and observed durations from planting to flowering (days after planting), durations from planting to maturity (days after planting), and grain yields of maize. The solid and dashed lines are the regression line and 1:1 line, respectively. The top row of panels shows the calibration results with one group of experimental data (n=12), and the bottom row of panels shows the validation results with another group of experimental data (n=23).

Table 3
Major genetic parameters adjusted for the six cultivars used in the study.

Cultivar	P1 (°C d)	P2	P5 (°C d)	G2 (kernels/plant)	G3 (mg d^{-1})	PHINT (°C d)
Zhedan37	210	0.7	670	800	8.6	38.9
Jidan180	250	0.7	830	830	8.5	38.9
Danyu39	220	0.7	1070	830	8.5	38.9
Nongda108	260	0.7	890	680	10	38.9
Zhengdan958	250	0.7	1030	820	8.2	38.9
Zhenghong505	250	0.7	1000	800	9.5	38.9

Note: P1, Thermal time from emergence to the end of the juvenile phase; P2, Photoperiod sensitivity coefficient; P5, Thermal time from silking to physiological maturity; G2, Maximum number of kernels per plant; G3, Potential kernel filling rate during the linear grain filling stage; PHINT: Thermal time required for a leaf tip to appear (based on 8°C d)

1.0 ha^{-1} (11.9%) for the validation period. The significant differences in genetic parameters between cultivars were thermal time from emergence to the end of the juvenile phase, and thermal time from silking to physiological maturity, maximum number of kernels per plant, and potential kernel filling rate (Table 3). Zhedan37 and Jidan 190 required less thermal time to mature than the other four maize cultivars. Nongda108 had lower maximum number of kernels but higher potential filling rate compared with the other maize cultivars.

3.2. *Climate change effects and adaptation potential to rising temperature and heat stress*

Climate change would have negative impacts on maize yield across China's Maize Belt if adaptation options were not considered (Figs. 4a and S3). On average, simulated yield would consistently decline by 25.3% in the 2050s and by 44.5% in the 2080s compared with the baseline period. In particular, region V (the second largest maize producing area in China) was projected to have the greatest yield loss, with 36.2% lower yield in the 2050s and 60.6% lower yield in the 2080s.

We evaluated the potential of different adaptation options to climate warming. Maize yield losses in the future could be effectively mitigated

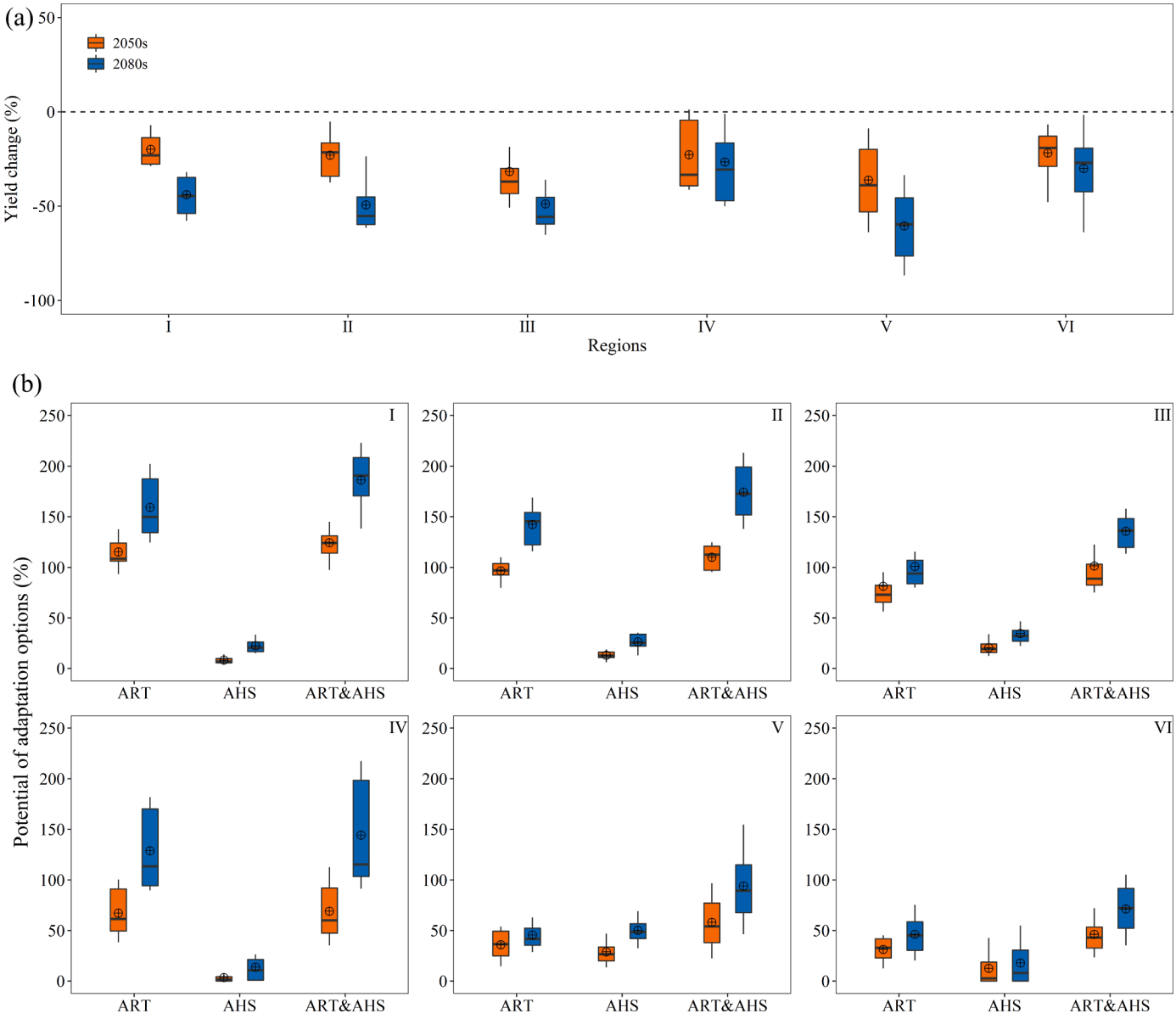

Fig. 4. The impact of climate change on rainfed maize yield (a), the potential for adapting to rising temperature (ART), the potential for adapting to heat stress (AHS), and the potential for adapting to both ART and AHS across six planting regions (b). Box boundaries indicate the 25th and 75th percentiles across sites in each region, whiskers below and above the box indicate the 10th and 90th percentiles, bars in boxes indicate the 50th percentiles, and crosshairs indicate mean values.

by using adapted cultivars to adapt to both rising temperature and heat stress (Fig. S4). Additionally, the simulated results showed that the potential for adapting to rising temperature was greater than the potential for adapting to heat stress in all regions except region V in the 2080s (Fig. 4b). For the regional estimates, the highest adaption potential to rising temperature would occur in region I with 115.1% in the 2050s and 165.2% in the 2080s. Conversely, the lowest adaptation potential to rising temperature was in region VI with 25.7% and 38.7% in the 2050s and the 2080s, respectively. In addition, the highest adaption potential to heat stress would occur in region V with 28.8% in the 2050s and 50.2% in the 2080s, while the lowest adaptation potential was in region IV with 3.9% and 15.6% in the 2050s and 2080s, respectively. As a result, adapting to both rising temperature and heat stress had the greatest potential for boosting maize yield across all regions.

3.3. Future adapted cultivars across China's Maize Belt

Given that the reference cultivars exhibited great yield loss in the future due to climate change (Fig. 4a), we recommend use of the adapted cultivars with optimal thermal time and temperature thresholds for China's Maize Belt in the 2050s and the 2080s (Fig. 5). For the baseline period, the optimal thermal time for adapted cultivars (P1+P5) only in region VI increased by 380°C d. However, in the other regions, the optimal thermal time for adapted cultivars (P1+P5) had slight changes compared with the reference cultivars. In contrast, the optimal thermal time for adapted cultivars (P1+P5) would have a large increase in the future compared with the baseline period. The greatest increase of thermal time (P1+P5) was projected in region III with 770 and 1160°C d in the 2050s and the 2080s, respectively (Fig. 5c), while the least increase was in region V with 380 and 640°C d in the 2050s and the 2080s,

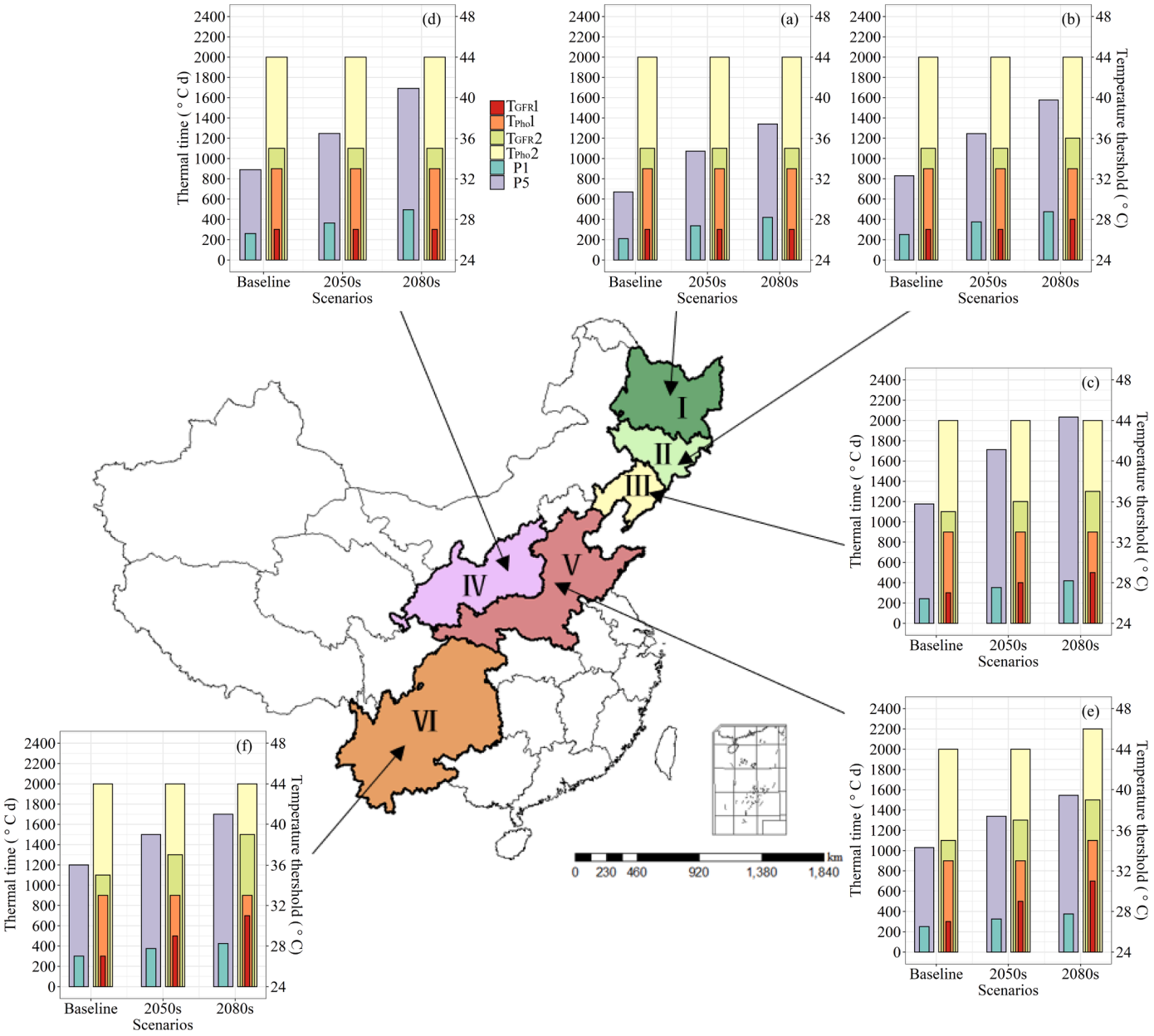

Fig. 5. Optimal thermal time and temperature thresholds for photosyntheis and grain filling rate across China's Mazie Belt for adapted cultivars that will mitigate adverse impacts of rising temperature and heat stress during the baseline period, the 2050s, and the 2080s. P1 represents the thermal time from emergence to end of the juvenile phase, and P5 represnets the thermal time from silking to physiological maturity. $T_{Pho}1$ and $T_{Pho}2$ represent the upper limits of optimal temperature and lethal temperature for photosynthesis, respectively. $T_{GFR}1$ and $T_{GFR}2$ represent the upper limits of optimal temperature and lethal temperature for grain filling rate, respectively.

respectively, compared with the baseline period (Fig. 5e).

The optimal temperature thresholds for grain filling rate ($T_{GFR}1$ and $T_{GFR}2$) would increase by 1°C during the 2080s in regions I–II (Fig. 5a and b) compared with the baseline period, and increase by 1°C during the 2050s and 2°C during the 2080s in region III (Fig. 5c). There was an increase of 2°C during the 2080s and 4°C during the 2080s for temperature thresholds for grain filling rate ($T_{GFR}1$ and $T_{GFR}2$) in regions V and VI (Fig. 5e and f). In contrast, the optimal temperature thresholds for photosynthesis ($T_{Pho}1$ and $T_{Pho}2$) would increase by 1°C only during the 2080s in region V (Fig. 5e).

Fig. 6 shows that the pre- and post-flowering periods of the current maize cultivars (averaged over the six planting regions) would be shortened by 6 and 19 days, respectively, during the 2050s, and shortened by 12 and 24 days during the 2080s. According to regional estimates, the whole growth period would be strongly shortened in region IV by 32 and 52 days (Fig. 6d), but shortened in region V by 18 and 25 days during the 2050s and the 2080s (Fig. 6e). As both periods would be shortened by rising temperature, optimizing thermal time for adapted cultivars should prolong both the pre- and post-flowering time (Fig. 6). After taking full advantage of the growth period by optimizing thermal time, the maize growth period for regions I–IV with the single-cropping system could be lengthened by 15 days in the 2050s and 30 days in the 2080s compared with the baseline period (Fig. 6a–d). Alternatively, the growth period in regions V and VI was the same as the growth period during the baseline period because the maize growing season was constrained by the following crop in the double-cropping system (Fig. 6e and f). From the above results, we suggest that the rising temperature would shorten the growth period. However, optimizing thermal time could mitigate this effect, and consequently achieve higher maize yield.

We compared the distributions of temperature during the whole growth period and the grain-filling period for maize cultivars with and without optimal thermal time during the baseline period, the 2050s, and the 2080s in the six regions (Fig. 7). Heat stress would increase with climate change in all regions, but with large spatial differences. Region V was largely affected by heat stress for both photosynthesis and grain filling rate compared with other regions. In particular, heat stress would impact maize photosynthesis only in region V during the 2080s (Fig. 7a–b), where the accumulated heat stress effect index was 0.2 for the adapted cultivar and 0.3 for the reference cultivar (Table S8). In contrast, heat stress for grain filling was more significant than for photosynthesis in all regions, though both grain filling and photosynthesis showed regional differences. Specifically, grain filling rate would be affected by heat stress more severely in regions III, V, and VI (Fig. 7c–d), with average accumulated heat stress impact factors of 0.17 and 0.22 during the 2050s, and 0.26 and 0.38 during the 2080s for adapted cultivars and the reference cultivars, respectively (Table S8). Lesser accumulated heat stress was found for adapted cultivars with higher thermal time compared with the reference cultivars, implying that optimizing thermal time would also alleviate accumulated heat stress impacts.

4. Discussion

We found that climate change will greatly decrease future maize yields across China's Maize Belt unless cultivars adapted to the changed climate are developed and used. This result is consistent with previous

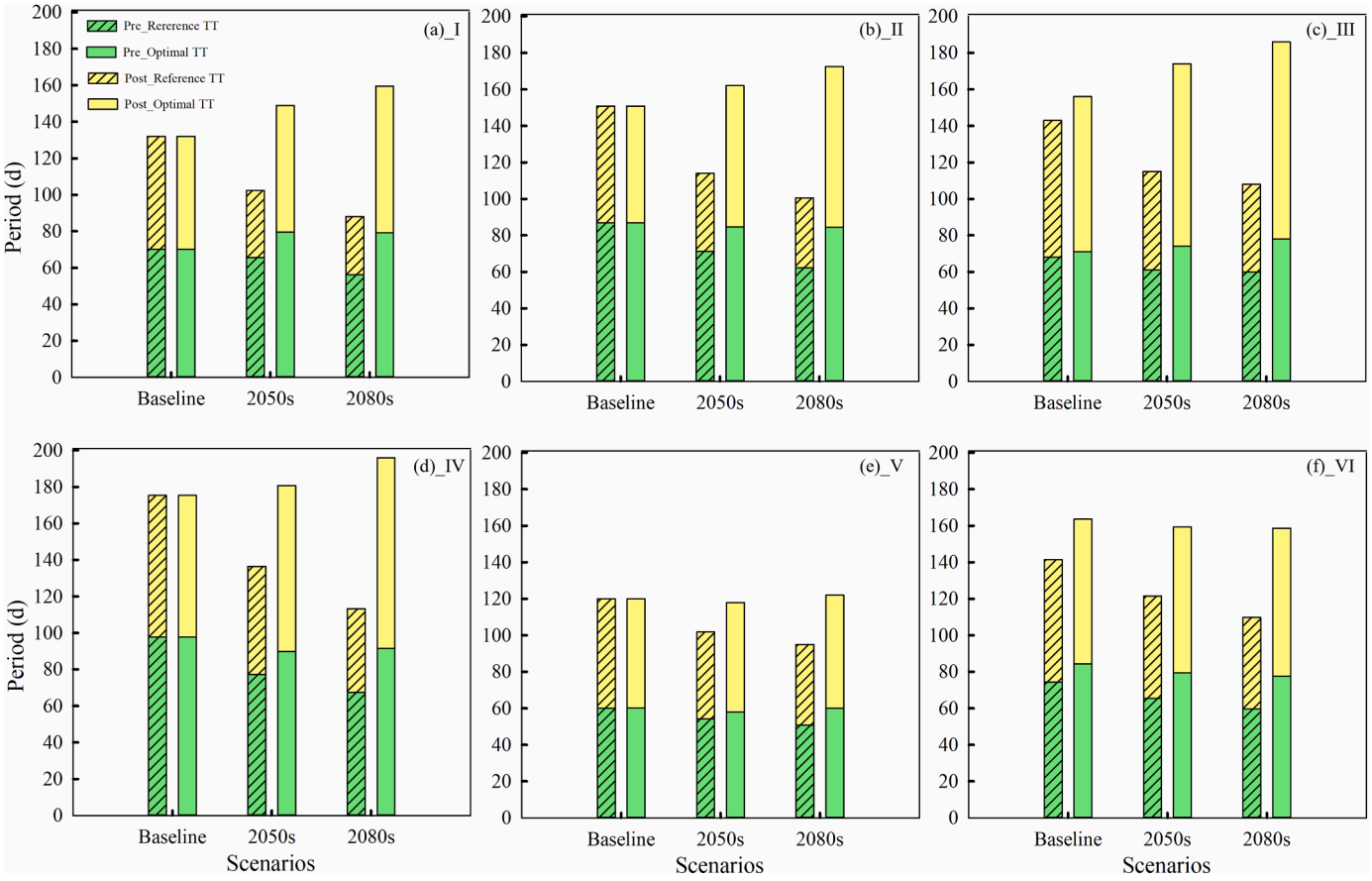

Fig. 6. Length of pre- and post-flowering periods for reference cultivars and adapted cultivars with optimal thermal time under different scenarios across six planting regions. "Pre_Reference TT" represents the pre-flowering period for the reference cultivar, and "Pre_Optimal TT" represents the pre-flowering period for the adapted cultivar with optimal thermal time. "Post_Reference TT" represents the post-flowering period for the reference cultivar, and "Post_Optimal TT" represents the post-flowering period for the adapted cultivar with optimal thermal time.

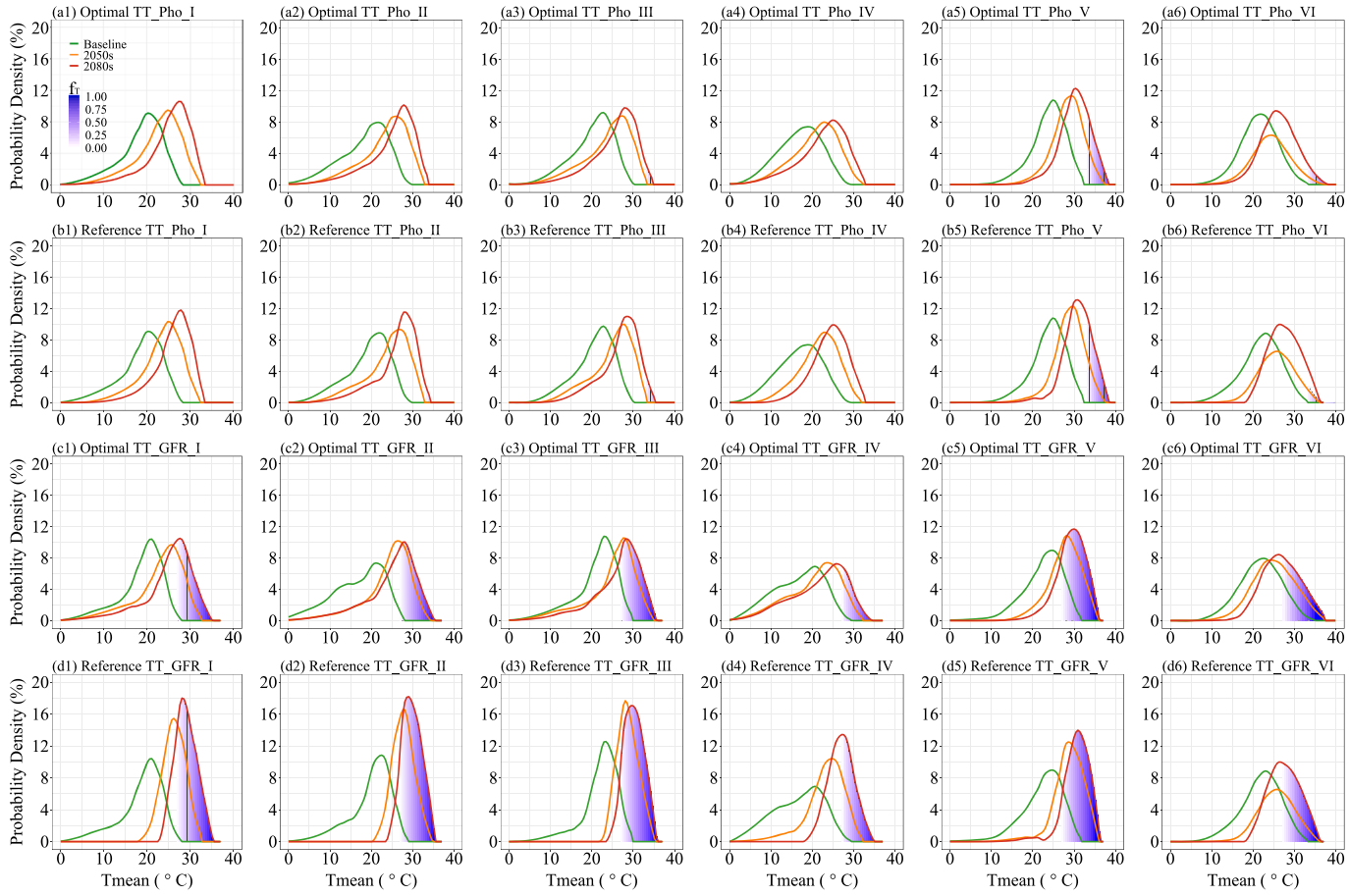

Fig. 7. Probability of different mean temperatures occurring during the whole growth period (a, b) and grain filling period (c, d). a1–a6, results for adapted cultivars with optimal thermal time (Optimal TT) and heat stress (f_T) effects on photosynthesis (Pho) in six maize planting regions during the baseline period, the 2050s, and the 2080s. b1–b6, results for reference cultivars with non-optimized thermal time (Reference TT) and f_T effects on Pho. c1–c6, results for adapted cultivars with Optimal TT and f_T effects on grain filling rate (GFR). d1–d6, results for Reference TT and f_T effects on GFR. The puple shadow represents the accumulated heat stress impact factor. (For interpretation of the references to colour in this figure legend, the reader is referred to the web version of this article.)

studies in different maize planting regions in China (Tao and Zhang, 2010; Xiong et al., 2007). Similar conclusions have been drawn in maize planting regions in the US, Africa, and other countries (Lobell et al., 2011b; Rosenzweig et al., 2013; Rurinda et al., 2015; Schauberger et al., 2017). However, compared with other climate change impact studies (Chen et al., 2018; Faye et al., 2018; Huang et al., 2020; Xiong et al., 2007), the magnitude of yield reduction in our study was greater as we used an extremely hot global climate model with mean temperature increasing by 4.4°C in the 2050s and by 6.4°C in the 2080s under SSP585 to explore the potential of adapted cultivars under the worst scenario. We found climate warming with rising temperature, and heat stress was the main factor resulting in yield losses in all regions due to the shortened growth period (Figs. S5 and S6). Region V exhibited the largest yield loss compared with other subregions. This is because there was a remarkably adverse effect of heat stress on maize yield (Fig. S5d5), and because the accumulated heat stress factor was greatest in the region V (Fig. S6d). Specifically, maize was mainly grown in June–September in region V, while in other regions the maize growing season was April/May–September (Table 1). Maize growing season temperatures in region V were 6.2, 5.0, 3.3, 5.8, and 1.3°C higher than those temperatures in region I, II, III, IV, and VI, respectively, during the baseline period (Table S1). In addition, temperatures during future maize growth periods were expected to increase by 3.8–8.8°C in region V (Fig. S6a). Therefore, heat stress would result in decreased maize yields in region V due to higher growth period temperatures in the future (Fig. S6a and d). In contrast, region VI is located in the area of lowest latitude, but the yield losses and adaption potential to rising temperature were lower than in region V (Fig. 4). This is because maize growing season temperature in region VI was lower than in region V (Table S1). In addition, a lower temperature increase in region VI was projected compared with other regions (Fig. S6a).

A previous study showed that the combination of adjusting planting date and selecting appropriate cultivars can offset the adverse effects of climate warming on maize yields under scenarios of 1.5°C and 2°C warming (Huang et al., 2020). However, under more severe warming, new cultivars need to be bred to address the more adverse effects of rising temperature and heat stress on maize yield (Xin and Tao, 2019; Zhang and Zhao, 2017). Our study assessed the relative potential of adapting to rising temperature and heat stress across China's Maize Belt using the climate-crop modelling approach. We found that the potential of adapting to rising temperature was generally higher than that of adapting to heat stress in most regions except region V during the 2080s (Fig. 4b). Based on this result, we suggest that targeting the adaptation to rising temperature has a higher priority than targeting adaptation to heat stress in most of China's maize planting regions.

The spatial differences in adaption potential are caused by various climate and cropping systems across China's Maize Belt. Specifically, maize growth periods in regions I–IV with a single-cropping system can be extended by adopting new cultivars with higher thermal time to fully utilize increased thermal resources (Chen et al., 2013; Zhao et al., 2015). However, for region V with a double-cropping system, maize growth period cannot be lengthened but can only be maintained as the current

length of the growth period is constrained by the next winter wheat crop (Huang et al., 2018). In addition, current growing season temperature has approached the optimal temperature for maize growth and development in region V where maize is more sensitive to heat stress under future climate change. Thus adaptation potential to heat stress is relatively higher than in other regions (Fig. 7).

To provide a robust reference for breeders, our study determined the optimal thermal time and temperature thresholds for adapted cultivars for the 2050s and the 2080s. The thermal time for adapted cultivars needs to be increased by 550°C d for the 2050s and by 900°C d for the 2080s averaged across China's Maize Belt, with the highest increase in region III (770 and 1160°C d during the 2050s and the 2080s, respectively) and lowest increase in region V (380 and 640°C d during the 2050s and the 2080s, respectively). A previous study showed that the thermal time gap between current maize cultivars used in China is 400°C d (Huang et al., 2020). Theoretically, it is possible to achieve such high thermal time under moderate warming conditions in the future.

To alleviate the effects of heat stress on maize yield, the optimal temperature threshold for maize grain-filling rate in region V is likely to be increased by 2°C during the 2050s and 4°C during the 2080s. Additionally, the optimal temperature threshold for photosynthesis will need an increase of 1°C only in the 2080s. In contrast, there is not much difference in temperature threshold change in the future for other regions (Fig. 5). Therefore, the responses of maize to heat stress vary depending on the particulars of the local climate. For instance, region V has the highest risk of heat stress (Fig. 7b5 and d5), while heat stress has minimal impacts in region IV (Fig. 7b4 and d4) in China's Maize Belt. However, our suggested optimal temperature threshold was based on crop model simulations. The impacts of heat stress on final grain yield are not just for photosynthesis and grain filling rate, but are more complex and diverse (Ellis et al., 1992; Eyshi Rezaei et al., 2015). Great challenges remain for us to incorporate the complicated mechanism of heat stress effects on crop physiology and biochemistry into biophysical crop models (Jin et al., 2016; Zhu et al., 2019). In fact, a large diversity in maize temperature thresholds among studies has been found. For example, the upper optimum temperature of maize photosynthesis ranges from 30 to 38°C (Crafts-Brandner and Salvucci, 2002; Luo, 2011), and the temperature for grain filling rate varies between 26.4 and 32°C (Commuri and Jones, 1999; Sanchez et al., 2014). Field experiments have shown that planting some tropical or subtropical maize varieties in temperate regions produced larger grain harvest than other varieties because they have high resistance to heat events (Rattalino Edreira and Otegui, 2013). Thus, breeding new cultivars or using existing heat-tolerant cultivars is important in the warmer regions of China's Maize Belt.

We also compared the impacts of heat stress on maize yield under rainfed and potential conditions and found similar results (Figs. 5 and S7). However, previous studies showed that heat stress had more adverse impacts on maize yield under water stress conditions because drought results in higher canopy temperatures than air temperature (Lobell et al., 2011a; Siebers et al., 2015). Therefore, using canopy temperature instead of air temperature would be better for evaluating the impacts of heat stress on maize (Siebert et al., 2017). However, the majority of presently available crop models do not consider canopy temperature as related to irrigation management.

There are some limitations to our study. First, in most process-based crop models including CERES-Maize, the effect of heat stress on maize yield is underestimated because the models use the daily mean temperature instead of daily maximum temperature to evaluate the impacts of heat stress on photosynthesis and grain filling rate (Jin et al., 2016; López-Cedrón et al., 2005). Instantaneous high temperature extremes (e.g., daily maximum temperature > 36°C) result in an irreversible impact on crop yield (Asseng et al., 2011; Hawkins et al., 2013). Second, our study only focused on a cultivar with appropriate adaptation traits, and did not consider the impact of other agronomic options (e.g., adjusting planting date and nitrogen application rate) on yield (Xiao et al., 2020b; Xin and Tao, 2019). Maize yield will have a greater increase if we optimize the Genotype (G) × Environment (E) × Management (M) interactions in order to propose optimal agronomic management practices and cultivars. Third, our study only used one crop model to simulate the impacts of climate warming on maize yield. Recent studies (Asseng et al., 2013; Asseng et al., 2014; Martre et al., 2015) found that an ensemble of multiple crop models was able to provide a more reliable climate change impact assessment than a single crop model. Further work is needed to assess the potential of different adaptation options to alleviate the effects of climate warming on maize yield by integrating multiple crop models and climate models (Trnka et al., 2014; Webber et al., 2018).

5. Conclusion

Our study explored the impact of rising temperature and heat stress on maize yield, and assessed maize adaptation potential across China's Maize Belt. We found that without cultivar adaptation, maize yield would decline by 25.3% and 44.5% during the 2050s and the 2080s, respectively, compared with the baseline period. With adaptation, the potential of adapting to rising temperature was higher than the potential of adapting to heat stress in all regions except region V during the 2080s. Region I would have the highest adaption potential to rising temperature, and region V would have the highest adaption potential to heat stress. The adapted cultivar in region III was projected to have the highest increase of thermal time compared with the adapted cultivars in other regions. The adapted cultivar in region V was projected to have the highest increase of optimal temperature thresholds for grain filling rate and photosynthesis. Our results demonstrate that the combination of increasing thermal time and optimizing temperature thresholds for maize cultivars can mitigate the adverse effects of extreme climate warming on China's maize yield. The study results will provide a scientific reference for future breeding of maize cultivars that are adapted to climate change.

Declaration of Competing Interest

The authors declare no conflict of interests.

Acknowledgements

The study was funded by the National Key Research and Development Program of China (2017YFD0300304), Central Public-Interest Scientific Institution Basal Research Fund of China (2020SYIAEZD3), CMA/Henan Key Laboratory of Agrometeorological Support and Applied Technique (AMF201905) and the Natural Science Foundation of Qinghai (2021-HZ-811). Mingxia Huang acknowledges that the Chinese Scholarship Council provided the scholarship and the NSW Department of Primary Industries provided office facilities for conducting this work (2019–2021). Thanks to Dr. Bernie Dominiak for his editing and internal review of the manuscript. We are grateful to two reviewers and editors for their thorough and helpful comments which greatly improved our manuscript.

Supplementary materials

Supplementary material associated with this article can be found, in the online version, at doi:10.1016/j.agrformet.2021.108673.

Reference

Abbas, G., et al., 2017. Quantification the impacts of climate change and crop management on phenology of maize-based cropping system in Punjab, Pakistan. Agric. For. Meteorol. 247, 42–55.

Araya, A., et al., 2015. Assessment of maize growth and yield using crop models under present and future climate in southwestern Ethiopia. Agric. For. Meteorol. 214-215, 252–265.

Asseng, S., et al., 2014. Rising temperatures reduce global wheat production. Nat. Clim. Change 5 (2), 143–147.
Asseng, S., et al., 2013. Uncertainty in simulating wheat yields under climate change. Nat. Clim. Change 3, 827–832.
Asseng, S., Foster, I.A.N., Turner, N.C., 2011. The impact of temperature variability on wheat yields. Glob. Change Biol. 17 (2), 997–1012.
Bai, H., et al., 2020. Multi-model ensemble of CMIP6 projections for future extreme climate stress on wheat in the North China plain. Int. J. Climatol. 41 (3), 171–186.
Ben-Ari, T., et al., 2018. Causes and implications of the unforeseen 2016 extreme yield loss in the breadbasket of France. Nat. Commun. 9 (1), 1627.
Braga, R.P., Cardoso, M.J., Coelho, J.P., 2008. Crop model based decision support for maize (*Zea mays* L.) silage production in Portugal. Europ. J. Agron. 28 (3), 224–233.
Cairns, J.E., et al., 2012. Maize production in a changing climate: impacts, adaptation, and mitigation strategies. Adv. Agron. 114, 1–58.
Challinor, A.J., Koehler, A.K., Ramirez-Villegas, J., Whitfield, S., Das, B., 2016. Current warming will reduce yields unless maize breeding and seed systems adapt immediately. Nat. Clim. Change 6 (10), 954–958.
Challinor, A.J., Wheeler, T.R., Craufurd, P.Q., Ferro, C.A.T., Stephenson, D.B., 2007. Adaptation of crops to climate change through genotypic responses to mean and extreme temperatures. Agric., Ecosyst. Environ. 119 (1-2), 190–204.
Chen, X., et al., 2013. Modern maize hybrids in Northeast China exhibit increased yield potential and resource use efficiency despite adverse climate change. Glob. Change Biol. 19 (3), 923–936.
Chen, Y., Zhang, Z., Tao, F., 2018. Impacts of climate change and climate extremes on major crops productivity in China at a global warming of 1.5 and 2.0 °C. Earth Syst. Dynam. 9 (2), 543–562.
Chisanga, C.B., Phiri, E., Chinene, V.R.N., 2020a. Reliability of rain-fed maize yield simulation using LARS-WG derived CMIP5 climate data at Mount Makulu, Zambia. J. Agric. Sci. 12, 275–289.
Chisanga, C.B., Phiri, E., Chinene, V.R.N., Chabala, L.M., 2020b. Projecting maize yield under local-scale climate change scenarios using crop models: Sensitivity to sowing dates, cultivar, and nitrogen fertilizer rates. Food Energy Secur. 9, 1–17.
Commuri, P.D., Jones, R.J., 1999. Ultrastructural characterization of maize (*Zea mays* L.) kernels exposed to high temperature during endosperm cell division. Plant Cell Environ. 22, 375–385.
Crafts-Brandner, S.J., Salvucci, M.E., 2002. Sensitivity of photosynthesis in a C-4 plant, maize, to heat stress. Plant Physiol. 129, 1773–1780.
Deryng, D., Conway, D., Ramankutty, N., Price, J., Warren, R., 2014. Global crop yield response to extreme heat stress under multiple climate change futures. Environ. Res. Lett. 9 (3), 034011.
Dou, P., et al., 2017. Effect of sowing date on dry matter accumulation and yield of maize in hilly regions of Sichuan Province, China. Chin. J. Eco Agric. 25, 221–229.
Ellis, R.H., Summerfield, R.J., Edmeades, G.O., Roberts, E.H., 1992. Photoperiod, temperature, and the interval from sowing to tassel initiation in diverse cultivars of maize. Crop. Sci. 32 (1), 1225–1232.
Eyshi Rezaei, E., Webber, H., Gaiser, T., Naab, J., Ewert, F., 2015. Heat stress in cereals: mechanisms and modelling. Europ. J. Agron. 64, 98–113.
FAO, 2017. Food and Agriculture Organization of the United Nations, Statistics Division. FAOSTAT. https://www.fao.org/faostat/en/#data/QCL (accessed 20 June 2019).
Faye, B., et al., 2018. Impacts of 1.5 versus 2.0 °C on cereal yields in the West African Sudan Savanna. Environ. Res. Lett. 13 (3), 034014.
Gourdji, S.M., Sibley, A.M., Lobell, D.B., 2013. Global crop exposure to critical high temperatures in the reproductive period: historical trends and future projections. Environ. Res. Lett. 8 (2), 024041.
Guan, K., Sultan, B., Biasutti, M., Baron, C., Lobell, D.B., 2017. Assessing climate adaptation options and uncertainties for cereal systems in West Africa. Agric. For. Meteorol. 232, 291–305.
Guo, H., et al., 2021. Assessment of CMIP6 in simulating precipitation over arid Central Asia. Atmos. Res. 252, 105451.
Han, Y., Gao, Y., Zheng, D., Du, J., 2016. Effects of meteorological factors on yield traits of maize (*Zea mays* L.) in Heilongjiang during various sowing seasons. Agric. Res. Arid Areas 34, 132–138.
Hawkins, E., et al., 2013. Increasing influence of heat stress on French maize yields from the 1960s to the 2030s. Glob. Change Biol. 19 (3), 937–947.
Huang, M., et al., 2020. Optimizing sowing window and cultivar choice can boost China's maize yield under 1.5°C and 2°C global warming. Environ. Res. Lett. 15 (2), 024015.
Huang, S., et al., 2018. Extending growing period is limited to offsetting negative effects of climate changes on maize yield in the North China Plain. Field Crops Res. 215, 66–73.
Huang, M., Wang, J., Wang, B., Liu, D.L., Yu, Q., He, D., et al., 2020. Optimizing sowing window and cultivar choice can boost China's maize yield under 1.5 °C and 2 °C global warming. Environ. Res. Lett. 15 (2), 024015.
IPCC, 2014. Summary for policymakers. In: Field, C.B., Barros, V.R., Dokken, D.J., Mach, K.J., Mastrandrea, M.D., Bilir, T.E., Chatterjee, M., Ebi, K.L.K.L., Estrada, Y.O., Genova, R.C., Girma, B., Kissel, E.S., Levy, A.N., MacCracken, S., Mastrandrea, P.R., White, L.L. (Eds.), Impacts, Adaptation, and Vulnerability. Part A: Global and sectoral aspects. Contribution of Working group II to the fifth assessment Report of the Intergovernmental Panel on Climate Change. Cambridge University Press, Cambridge, UK/New York, NY.
Jin, Z., et al., 2016. Do maize models capture the impacts of heat and drought stresses on yield? Using algorithm ensembles to identify successful approaches. Glob. Change Biol. 22 (9), 3112–3126.
Jones, J.W., et al., 2003. The DSSAT cropping system model. Europ. J. Agron. 18, 235–265.
Kang, S., Eltahir, E.A.B., 2018. North China Plain threatened by deadly heatwaves due to climate change and irrigation. Nat. Commun. 9 (1), 2894.
Li, L., et al., 2019. Future projections of extreme temperature events in different sub-regions of China. Atmos. Res. 217, 150–164.
Lin, Y., et al., 2017. Potential impacts of climate change and adaptation on maize in Northeast China. Agron. J. 109 (4), 1476–1490.
Liu, D.L., et al., 2017. Effects of different climate downscaling methods on the assessment of climate change impacts on wheat cropping systems. Clim. Change 144 (4), 687–701.
Liu, D.L., Zuo, H., 2012. Statistical downscaling of daily climate variables for climate change impact assessment over New South Wales, Australia. Clim. Change 115 (3-4), 629–666.
Lizaso, J.I., et al., 2018. Impact of high temperatures in maize: phenology and yield components. Field Crops Res. 216, 129–140.
Lobell, D.B., Bänziger, M., Magorokosho, C., Vivek, B., 2011a. Nonlinear heat effects on African maize as evidenced by historical yield trials. Nat. Clim. Change 1 (1), 42–45.
Lobell, D.B., Schlenker, W., Costa-Roberts, J., 2011b. Climate trends and global crop production since 1980. Science 333, 616–620.
López-Cedrón, F.X., Boote, K.J., Ruíz-Nogueira, B., Sau, F., 2005. Testing CERES-Maize versions to estimate maize production in a cool environment. Europ. J. Agron. 23 (1), 89–102.
Luo, Q., 2011. Temperature thresholds and crop production: a review. Clim. Change 109 (3-4), 583–598.
Martre, P., et al., 2015. Multimodel ensembles of wheat growth: many models are better than one. Glob. Change Biol. 21 (2), 911–925.
Rattalino Edreira, J.I., Otegui, M.E., 2012. Heat stress in temperate and tropical maize hybrids: differences in crop growth, biomass partitioning and reserves use. Field Crops Res. 130, 87–98.
Rattalino Edreira, J.I., Otegui, M.E., 2013. Heat stress in temperate and tropical maize hybrids: a novel approach for assessing sources of kernel loss in field conditions. Field Crops Res 142, 58–67.
Rosenzweig, C., et al., 2013. Assessing agricultural risks of climate change in the 21st century in a global gridded crop model intercomparison, 111. PNAS, pp. 3268–3273.
Ruane, A.C., et al., 2013. Climate change impact uncertainties for maize in Panama: Farm information, climate projections, and yield sensitivities. Agric. For. Meteorol. 170, 132–145.
Rurinda, J., et al., 2015. Climate change and maize yield in southern Africa: what can farm management do? Glob. Change Biol. 21 (12), 4588–4601.
Sanchez, B., Rasmussen, A., Porter, J.R., 2014. Temperatures and the growth and development of maize and rice: a review. Glob. Change Biol. 20 (2), 408–417.
Schauberger, B., et al., 2017. Consistent negative response of US crops to high temperatures in observations and crop models. Nat. Commun. 8, 13931.
Siebers, M.H., et al., 2015. Heat waves imposed during early pod development in soybean (*Glycine max*) cause significant yield loss despite a rapid recovery from oxidative stress. Glob. Change Biol. 21 (8), 3114–3125.
Siebert, S., Webber, H., Zhao, G., Ewert, F., 2017. Heat stress is overestimated in climate impact studies for irrigated agriculture. Environ. Res. Lett. 12 (5), 054023.
Singh, P., et al., 2014. Quantifying potential benefits of drought and heat tolerance in rainy season sorghum for adapting to climate change. Agric. For. Meteorol. 185, 37–48.
Swart, N.C., et al., 2019. The canadian earth system model version 5 (CanESM5.0.3). Geosci. Model Dev. 12 (11), 4823–4873.
Tao, F., Zhang, S., Zhang, Z., Rotter, R.P., 2014. Maize growing duration was prolonged across China in the past three decades under the combined effects of temperature, agronomic management, and cultivar shift. Glob. Change Biol. 20 (12), 3686–3699.
Tao, F., Zhang, Z., 2010. Impacts of climate change as a function of global mean temperature: maize productivity and water use in China. Clim. Change 105 (3-4), 409–432.
Tesfaye, K., et al., 2016. Climate change impacts and potential benefits of heat-tolerant maize in South Asia. Theor. Appl. Climatol. 130 (3-4), 959–970.
Trnka, M., et al., 2014. Adverse weather conditions for European wheat production will become more frequent with climate change. Nat. Clim. Change 4 (7), 637–643.
UN_DESA, 2017. United Nations, Department of Economic and Social Affairs, Population Division. World population prospects: The 2017 revision, key findings and advance tables. ESA/P/WP/248. https://population.un.org/wpp/Publications/Files/WPP2017_KeyFindings.pdf.
van Vliet, J., Eitelberg, D.A., Verburg, P.H., 2017. A global analysis of land take in cropland areas and production displacement from urbanization. Glob. Environ. Change 43, 107–115.
Wang, F., et al., 2020. Comprehensive evaluation of hydrological drought and its relationships with meteorological drought in the Yellow River basin, China. J. Hydrol. 584, 124751.
Wang, J., Wang, E., Yin, H., Feng, L., Zhao, Y., 2015. Differences between observed and calculated solar radiations and their impact on simulated crop yields. Field Crops Res. 176, 1–10.
Webber, H., et al., 2018. Diverging importance of drought stress for maize and winter wheat in Europe. Nat. Commun. 9 (1), 4249.
Webber, H., et al., 2017. Canopy temperature for simulation of heat stress in irrigated wheat in a semi-arid environment: A multi-model comparison. Field Crops Res. 202, 21–35.
Xiao, D., et al., 2020a. Climate change impact on yields and water use of wheat and maize in the North China Plain under future climate change scenarios. Agric. Water Manag. 238, 106238.
Xiao, D., Liu, D.L., Wang, B., Feng, P., Waters, C., 2020b. Designing high-yielding maize ideotypes to adapt changing climate in the North China Plain. Agr. Syst. 181, 102805.

Xin, Y., Tao, F., 2019. Optimizing genotype-environment-management interactions to enhance productivity and eco-efficiency for wheat-maize rotation in the North China Plain. Sci. Total Environ. 654, 480–492.
Xiong, W., Matthews, R., Holman, I., Lin, E., Xu, Y., 2007. Modelling China's potential maize production at regional scale under climate change. Clim. Change 85 (3-4), 433–451.
Yakoub, A., Lloveras, J., Biau, A., Lindquist, J.L., Lizaso, J.I., 2017. Testing and improving the maize models in DSSAT: Development, growth, yield, and N uptake. Field Crops Res. 212, 95–106.
Yazdandoost, F., Moradian, S., Izadi, A., Aghakouchak, A., 2021. Evaluation of CMIP6 precipitation simulations across different climatic zones: Uncertainty and model intercomparison. Atmos. Res. 250, 105369.
Zhang, Y., Zhao, Y., 2017. Ensemble yield simulations: Using heat-tolerant and later-maturing varieties to adapt to climate warming. PLoS One 12 (5), 0176766.
Zhao, J., Yang, X., Dai, S., Lv, S., Wang, J., 2015. Increased utilization of lengthening growing season and warming temperatures by adjusting sowing dates and cultivar selection for spring maize in Northeast China. Europ. J. Agron. 67, 12–19.
Zhu, P., Zhuang, Q., Archontoulis, S.V., Bernacchi, C., Muller, C., 2019. Dissecting the nonlinear response of maize yield to high temperature stress with model-data integration. Glob. Change Biol. 25 (7), 2470–2484.